Proceedings World Geothermal Congress 2000
Kyushu - Tohoku, Japan, May 28 - June 10, 2000

CHEMICAL AND THERMAL CHANGES IN THE ALUTO-LANGANO GEOTHERMAL FIELD , ETHIOPIA: FROM FLUID INCLUSION STUDY

Meseret Teklemariam
Ethiopian Institute of Geological Surveys
Hydrogeology, Engineering geology and Geothermal Department
P.O.Box, 40069, Addis Ababa, Ethiopia

Key words: Ethiopia, geothermal field, fluid inclusion

ABSTRACT
The study of fluid inclusions at the Aluto-Langano geothermal field has demonstrated the existence of a complex evolution of the geothermal fluids from the early stages of geothermal activity up to the present day. Evidence of heating in the upflow zone (wells LA-3 and LA-6) of the system is provided by a comparison of the present in-hole temperature (320-335°C) with the average fluid inclusion homogenization temperature (T_h= 240-330°C). On the other hand, in the lateral outflow zone of the system, in-hole temperatures are found to be about 176°C lower than the average homogenization temperatures indicating the occurrence of a strong cooling process after fluid inclusion formation.

Evidence for the change of compositions of fluids has been documented by the microthermometric data where the earlier fluids, responsible for the fluid inclusion formation, are more saline and less rich in CO_2 content in comparison with the present reservoir fluid. The apparent salinities of the fluid inclusions, estimated from the ice-melting temperature (0.0-3.1 wt% NaCl eq.) are, in most cases, higher than the salinity of the present reservoir fluid (0.1-0.4 wt% NaCl eq.).

Crushing experiments have shown that the dissolved CO_2 content in the Aluto-langano inclusions is variable. Most of the crushed inclusions from wells LA-3 and LA-6 contain a CO_2 amount (<0.05 m) lower than those present in the discharge fluid (0.11-0.21 m). On the other hand, the CO_2 content of most of the inclusions from wells LA-4, LA-7 and LA-8 is found to be higher than 0.08 m; the absence of clathrate during freezing runs limits the maximum CO_2 content in these inclusions to 0.85 m(Hedenquist and Henley, 1985). The T_{mi} - T_h distribution suggests the occurrence of both boiling and dilution processes in the Aluto-Langano geothermal system.

1. INTRODUCTION

The Aluto-Langano geothermal field is located about 200 km south of Addis Ababa (Fig.1), close to the eastern margin of the Ethiopian Rift and well inside the presently active axis of the Rift, i.e. the Wonji Fault Belt (WFB;). It is a high-temperature (335°C), water-dominated gas rich geothermal field hosted by peralkaline rhyolitic lavas and ignimbrites as well as transitional to alkaline basalts.

At Aluto, eight deep exploratory wells were drilled, five of which are productive. Exploratory and production wells identified an upflow zone (wells LA-3 and LA-6) with temperatures of 300-335°C and partial pressures of CO_2 of the order of 1.3 MPa. The zone of lateral outflow is characterizedby more diluted waters with temperatures in the range of 150-270°C, local temperature inversions at the margins of the field and very high PCO_2 (3-5 MPa). This geothermal field is currently in development stage where the five productive wells are supplying sufficient steam to operate a power plant of 5-7 Mwe, already connected to the national grid. The aim of the present study is to reconstruct the physical and chemical evolution of the discharge fluid and to identify the variations in the thermal regime of the Aluto-Langano geothermal field.

1.1 Fluid chemistry and Hydrothermal alteration mineralogy

The chemical composition of fluids produced by hot springs, shallow and deep wells belong to an alkali-bicarbonate chloride water, with pH that is near neutral to slightly alkaline(Teklemariam et al., 1996). The geothermal wells produce a two-phase fluid (water+vapour) with a total flow rate in the range of 10.4-25.6 Kg/sec and have enthalpy values in the range of 970-1650J/g. The computed chemical composition of the liquid fraction of the reservoir is reported in Table 1.

In the upflow zone, the hydrothermal mineral assemblage is characterized by the presence of calc-silicate minerals such as (epidote, garnet, prehnite and actinolite). However, these phases also occur as relics in wells where low temperatures are measured (Teklemariam, 1996). Calcite, quartz, adularia, pyrite, hematite and chlorite are widespread minerals in all wells, both at low and high temperatures.

2. FLUID INCLUSION STUDIES

2.1 Materials and methods used

Core samples from wells LA-3, LA-4, LA-6, LA-7 and LA-8 were petrographically examined in order to find suitable crystals for fluid inclusion studies.

The microthermometric measurements were carried out on doubly polished wafers (200-300 μm) using a heating and freezing CHAIXMECA stage (Poty et al, 1976) at the laboratory of International Institute for Geothermal Research, Pisa, Italy. Calibration for the freezing measurements was by the use of CO_2-H_2O and pure H_2O fluid inclusions, and for the heating measurements by the use of chemical products of known melting temperatures. The accuracy of the microthermometric measurements, based on repeated measurements, is estimated to be 0.1 °C at temperature below 0 °C and 1.5°C for homogenization temperatures.

2.2 Fluid inclusion types and their distribution

The fluid inclusions studied are mostly hosted by hydrothermal quartz and calcite that usually occur as vein cavity and vesicle fillings. Although the majority of fluid inclusion measurements were made on hydrothermal quartz and calcite, secondary inclusions suitable for study have also been found in magmatic quartz .

The fluid inclusions occur as primary, pseudosecondary and secondary inclusions. Primary inclusions were mostly recognized along growth surfaces in quartz crystals (Fig.2a) whereas secondary and pseudosecondary fluid inclusions are widely distributed along healed microfractures (Figs..2b and 2c). The inclusions are generally small in size, with a maximum length of 30 μm. They are negative crystal shaped, but also tubular or dendritic (the secondary ones only). The vast majority of the inclusions observed in the samples are aqueous two-phase liquid rich with liquid/vapour ratio of 80-90% (Figs 2a -c). However, less common two-phase (L+V) vapour rich or apparently one-phase (V) inclusions, and sometimes polyphase liquid rich inclusions are also observed.

2.3 Analytical results

Crushing experiments

Crushing experiments were performed in order to determine the non-condensable gas content semi-quantitatively (Sasada, 1985; Sasada et al.,1986), using a microscope crushing stage (Roedder, 1970). The method is based on the observation of the bubble behaviour when an inclusion is opened under applied pressure.

During freezing measurments, phenomena related to the presence of CO_2 such as CO_2 melting and clathrate formation were not observed within the studied inclusions. The minimum CO_2 content for clathrate formation is 0.83 m (Hedenquist and Henley, 1985; Sasada, 1985). A crushing test is a very sensitive and simple method to determine the presence of very small amount (0.08mol) of non-condensable gases in fluid inclusions. Since CO_2 is the main non-condensable gas in most geothermal fields, the CO_2 content may be approximately determined from the bubble behaviour on crushing (Sasada, 1985).

The bubble behaviour on crushing and estimated CO_2 content (Sasada et al., 1986) for inclusions from wells LA-4, 7 and 8 (present study) and wells LA-3 and LA-6 (Valori et al.,1992) are reported in Tables 2. Crushing experiments were carried out on chips selected from samples generally studied by microthermometry.

Bubble behaviour was observed in suitable liquid and vapour rich inclusions. Most of the bubble inclusions from wells LA-3 and LA-6 begin to shrink under applied pressure, followed by collapse and complete disappearance into the liquid (Table 2). This type of behaviour indicates the absence of appreciable amount of non-condensable gases, and as a consequnce, T_{mi} can be directly converted to weight percent of NaCl equivalent for most of the fluid inclusions that do not show any expansion behaviour. On the other hand, most of the bubble inclusions from wells LA-4, 7 and 8 expand and completely fill the cavity, indicating a pressure greater than atmospheric pressure and the presence of volatile components within the inclusions (Table 2). The gas phase in the inclusions is assumed to be mainly CO_2, based on the chemistry of the discharge fluid (Table1). According to Sasada et al (1986), the maximum CO_2 concentration possible for inclusions showing bubble collapse is 0.08 mole % (0.04 m);while, the minimum content for inclusions showing bubble expansion and cavity filling is 0.17 mole% (0.08 m).

Limited laser Raman spectroscopic analyses were performed for both vapour and liquid rich inclusions, but most of them were below detection limits (depending on compound and density). However, a very low concentration of CO_2 was observed in secondary liquid rich inclusions from wells LA-4 (1660 m) and LA-7 (2040 m).

Microthermometric results

The microthermometric data from the deep wells of Aluto are analysed below in terms of "cooling" and "heating." The fluid inclusion data for wells LA-3 and LA-6 which are discussed below are taken from Valori et al (1992).

Cooling data: Final ice melting-point measurements were made on 453 liquid rich inclusions. For very small inclusions (5-7μ m in length), the melting ice temperature (T_{mi}) was taken at the moment of last movement of the released bubble. Repeated runs on the same inclusion leads to uncertainity of 0.1°C in the T_{mi} measurements. During cooling runs, down to about -100 °C, phenomena related to the presence of CO_2 such as clathrate formation and CO_2 melting (-56.6 °C) were not observed. Although the vapour inclusions were routinely cooled to determine if they contained gases other than water, it was not possible to detect any phase change in them.

Ice melting temperatures (T_{mi}) ranges from -0.2 to -1.4°C for incluions in well LA-4; -0.2 to -1.8°C in well LA-7; and -0.3 to -1.6°C in well LA-8 (see Table 3). In the case of wells LA-3 and LA-6 T_{mi}, they range from -0.2 to -1.9°C and 0.0 to -1.9 °C, respectively

Heating data: The widest homogenization temperature (T_h) range and their bimodal and/or polymodal frequency distribution reflect the different generations of inclusions (i.e, fluid inclusions have formed at different times and P-T conditions). The homogenization temperatures (T_h) of 463 liquid rich inclusions were measured. All the measured inclusions homogenized in the liquid phase, and the uncertainity of the measurement is 1.5°C. T_h of vapour inclusions have not been determined, because none were suitable for accurate determination.

The homogenization temperatures for primary, pseudosecondary and secondary inclusions range from 201 to 309°C in well LA-4; 215 to 335 °C in well LA-7; and 214 to 330°C in well LA-8 (see Table 3). The T_h for wells LA-3 and LA-6 range from 242-347°C and 243-351°C, respectively. The frequency distribution of T_h for inclusions from wells LA-4, 7 and 8 are depicted in Figs 3a.,b and c, respectively. Assuming that pressure is hydrostatic and there is no change of water table since the time of trapping, the applied pressure correction is found to be <10°C, and the T_h is assumed to be close to the trapping temperature.

3. DISCUSSION

The interpretative framework of the fluid inclusion data will be discussed below in the form of (1) T_{mi} and the effect of NaCl and CO_2; (2) changes of fluid composition; (3) pressure-temperature conditions; and (4) T_{mi}-T_h relationships.

3.1 T_{mi} and the effect of NaCl and CO_2

The ice melting temperature for the studied inclusions ranges from -0.2 to -1.9, which is equivalent to 0.3 to 3.1 wt %NaCl eq.(Table 3). However, inclusions in Aluto-Langano

geothermal system would be expected to have measured ice melting temperature (T_{m-ms}) values of about -0.2 °C, on the basis of present salinity of the reservoir fluid (0.1-0.2 Wt % NaCl eq.). This is clearly not the case, with measured melting points ranging down to -1.9°C. The difference might be due to the presence of dissolved CO_2 which can contribute to the freezing point depression of the fluid. This case is also observed in the higher gas geothermal systems of Broadlands and Nghawa, New Zealand (Hedenquist, 1990); where, T_{m-ms} values and T_{m-cc} values are in between about -0.4°C and -2.0°C. The latter is due to a CO_2 concentration of about 1 m.

In fact, dissolved CO_2 might make a relatively large contribution to the depression of the melting point of dilute fluids, suggesting apparent salinities much higher than are actually present. In geothermal fluids, CO_2 dominates the dissolved gases, and in some systems (e.g. Nghawa and Broadlands, NewZealand), it is also the major dissolved component, its concentration exceeding that of chloride. Hedenquist and Henley (1985) proposed that the interpretation of ice melting point measurements can be erroneous if the CO_2 content of the fluid inclusion is not taken into account in the calculation of salinity. Therefore, variations in the ice melting temperatures of low salinity inclusions can result from differences in their gas contents since dissolved gases will also affect the freezing point depression.

A comparison between the calculated final ice melting temperatures on the basis of the chemical compositions of the discharge fluids (T_{m-cc}) and the measured ice melting temperatures (T_{m-ms}) is reported in Table 3. The chemical composition of the liquid fraction of the reservoir fluid computed by using Watch1 programme is also reported in Table 1. The discharge fluids from Aluto wells have a range of salinities (0.04-0.07 m total dissolved electrolytes, equiva-lent to 0.1-0.2 wt % NaCl eq.) and gas concentrations (0.12-0.50 m CO_2 plus other minor gases; see Table 1). T_{mi-cc} data from the total discharge compositions (electrolytes and nonelectrolytes) of Aluto wells from which fluid inclusion samples were available for examination has been calculated by using the equation proposed by Hedenquist and Henley (1985).

The mean apparent salinity of the fluid inclusions, calculated directly from the T_{mi} data for Aluto wells fall in the range of 0.8 -2.3 wt % NaCl eq.., which is substantially higher than the present salinity of the reservoir fluid. Assuming that the salinity of the geothermal fluid has remained constant, and that the gas consists dominantly of CO_2 as indicated in Table 1, the CO_2 content of the earlier fluid has been calculated using ΔT_{mi} (the difference between the actual measured ice melting temperature for inclusions and the calculated ice melting temperature on the basis of total dissolved electrolytes ($T_{m-cc,el}$). As is shown in Table 3, in most cases, the calculated CO_2 content of the earlier fluid is found to be higher than the CO_2 content of the present reservoir fluid. Only in the case of well LA-4, the CO_2 content of the present reservoir fluid (0.5 m) is found to be higher than the average calculated CO_2 (0.35 m; see Table 3).

In the case of wells LA-3 and LA-6, most of the studied inclusions indicate the absence of CO_2 in the earlier fluids, responsible for fluid inclusion formation; while, very few inclusions reveal the concentration of CO_2 in the range of 0.06 m < CO_2 <0.85 m. This estimation is based on the minimum concentration of CO_2 to form clathrate (0.85 m; Sasada et al., 1986) and detection limit of the spectroscopy (0.06 m). Besides, the estimated CO_2 concentration of the earlier fluid on the basis of the stability field of Calc-silicate mineral assemblages is found to be lower than 0.08 m (Teklemariam, 1996). Therefore, inclusions which have relatively lower T_{mi} from wells LA-3 and LA-6 might be due to the presence of dissolved salts, and hence the contribution of CO_2 for the freezing point depression is minimal.

Most of the bubbles of the inclusions from wells LA-4, 7 and 8 show expansion behaviour, indicating the presence of non-condensable gases. However, none of the studied inclusions show clathrate formation during microthermomeric measurements. Therefore, the concentration of CO_2 in these studied inclusions might be in the range of 0.08 m < CO_2 <0.83 m. In this case, the difference between the T_{mi-cc} and T_{mi-ms} can be explained by the fact that the fluid inclusions from these wells could contain higher amounts of CO_2 (or dissolved salts or both) in comparison with the present discharge fluid. However, the very low gas content of the fluid inclusions from wells LA-3 and LA-6 suggest that the CO_2 concentrations even in fluid inclusions from wells LA-4, 7 and 8 should not be very high (probably not higher than the CO_2 concentration in the present discharge fluid). Therefore, the difference between T_{mi-cc} and T_{m-ms} could possibly be explained due to the higher salinity of the fluid.

3.2 Changes of fluid composition

As is discussed in the previous section, the earlier hydrothermal fluids responsible for fluid inclusion formation may have had fluids of greater salinity than the present discharge fluid . This could be explained by the occurrence of a mixing processes , after trapping of fluid inclusions, where the higher saline fluid mixed with meteoric water. This mixing process is supported by the chloride-enthalpy diagram (Gianelli and Teklemariam, 1993) and Na-K-√Mg triangular diagram (Teklemariam, 1996), where all the discharge fluids from the Aluto wells fall along the dilution line. As a result, none of the discharge fluids could be representative of the parent reservoir fluid.

Raman spectroscopic analysis indicate the absence of CO_2 in most of the studied inclusions while very few of them (LA-4/1660 m; LA-7/2040 m) show a CO_2 content in the range of 0.06 m < CO_2 < 0.85 m. The result is consistent with the observation made by microthermometric studies where no clathrate formation and CO_2 melting is observed, and by crushing studies where most of the inclusions show a collapsing behaviour.

The concentration of CO_2 in the present reservoir fluid of wells LA-3 and LA-6 (0.11-0.21 m) is much higher than the earlier fluid that is responsible for the fluid inclusion formation (0.06 m < CO_2 < 0.83 m). On the other hand, the reservoir fluids of wells LA-4, 7 and 8 contain 0.13-0.50 m of CO_2 which is comparable with the range of CO_2 content of the studied inclusions (0.08 m < CO_2 < 0.83 m) estimated on the basis of microthermometric measurements and crushing studies. The lower limit for the past CO_2 concentration of the reservoir fluid is fixed by the stability field of the Ca-Al silicate mineral assemblages; where, a PCO_2 less than 10 bar (<0.08 m) is needed to reach in equilibrium at the time of mineral

deposition (Teklemariam, 1996). This fact is also observed in other geothermal fields such as Broadlands, New Zealand (Hedenquist, 1990); where, the CO_2 concentration in fluid inclusion is found to be much lower than the present discharge fluid. The increment of CO_2 concentration in the present reservoir fluid might be due to the intake of a CO_2 rich fluid in the geothermal reservoir which has the effect of destabilizing the mineral phases formed by the previous water-rock interaction processes.

3.3 Pressure-Temperature Conditions

Homogenization temperature of fluid inclusions provide some useful insights into the thermal regime at Aluto-Langano geothermal field. A comparison of T_h data with in-hole temperature and pressure profiles, once obtained, improves the interpretation of subsequent T_h measurement in the same system and indicates the thermal evolution of the system with time. The T_h-depth profiles will help determine where the fluid in a system was boiling, where mixing and conductive cooling occurred, and possibly the level of the paleo-water table (if the system was boiling; Hedenquist et al., 1992). Subtracting the mean fluid inclusion temperature from the present measured temperature (ΔT) at a given depth will indicate whether the local system has been heating or cooling since inclusion formation (Table 3). If a hydrostatic regime is considered at the time of trapping, the homogenization temperatures can be considered to be near the actual trapping temperature.

Thermal profiles in geothermal wells are often limited by the boiling point vs depth curve appropriate for the fluid composition (i.e. salinity and gas content). If the actual measured temperature profile deviates from the Boiling Point Curve for Pure Water (B.P.C.W) and if the concentration of CO_2 in the fluid is known from the composition of discharge fluid, it is possible to draw a B.P.C.with gas content (CO_2) of the discharge fluid.

Based on this approach, the relation of T_h and B.P.C.W (Haas, 1971) for primary, pseudosecondary and secondary inclusions from wells LA-4, 7 and 8 are shown on Figs.3a,b, and c respectively, and for wells LA-3 and 6, are reported on Valori et. al, 1992. The boiling point curves are adjusted to 100°C at the inferred current water table. Temperature profiles were measured after a 3-month heating-up period (Geothermal division data file). Figures 3 a, b and c depict the relation of T_h and boiling point curves for pure water (Haas, 1971) and for a mixture of H_2O-CO_2 with a CO_2 content of 1 mole % (0.5 m; the actual CO_2 content in the discharge fluid; Table 3).

The interpretation of T_h data based on pressure-temperature changes will be discussed in the form of (a) upflow zone (wells LA-3 and LA-6); (b) lateral outflow zone (wells LA-4 and LA-7), and (c) well LA-8.

(a) upflow zone (wells LA-3 and LA-6)

In the zone of upflow, the homogenization temperatures recorded for inclusions are found to be generally lower than, and in some cases equal to, the present day measured temperatures (Valori et al., 1992). In these wells, a comparison between the homogenization temperature and in-hole temperature indicates a heating up of the field. This might be due to an intake of a high enthalpy superheated fluid to the system. This heating condition is also registered in other geothermal fields such as Tongonan, Phillipines (Reyes, 1990).

(b) Lateral outflow zone (Wells LA-4 and LA-7)

Evidence of a cooling trend in wells LA-4 and LA-7 is provided by a comparison of the average homogenization temperatures and the present in-hole temperature (see Table 3; and Figs. 3a &b). In-hole measured temperatures are found to be up to 176°C lower than during fluid inclusion formation. However, a comparison of the microthermometric data (T_h and T_{mi}) with the present temperature and the calculated T_{mi} for the geothermal fluid indicate that only the fluid from the primary and secondary inclusions in calcite and quartz crystals at a depth of 1001 m (well LA-4) is similar to the present discharge fluid.

In the case of well LA-7, the homogenization temperatures of all primary, pseudosecondary and secondary inclusions are found to be higher than the present in-hole temperature, indicating the occurrence of a cooling process after fluid inclusion formation (Fig..3b). The association of a large thermal inversion with the majority of cooling in the lateral outflow zone of the system, suggests that incursion of marginal waters is the cause of cooling. This is similar to the Krishima geothermal system (Taguchi and Hayashi, 1983), where the focus of activity has shifted (associated with a drop in the upper surface of the geothermal water in a high relief terrain), resulting in as much as 100°C of cooling locally. This is also consistent with the progressive cooling at Broadlands, New Zealand around the margins (Hedenquist, 1990).

The presence of vapour rich inclusions coexisting with liquid rich inclusions in wells LA-4 and LA-7 indicate the occurrence of boiling at some time in the system. In well LA-4, all the recorded T_h values fall in the field of liquid with respect to the B.P.C.W except the primary inclusions in quartz crystal at 1250 m depth. The boiling condition at depths of 1001 m and 1660m and for the secondary inclusions in calcite at 1250 m depth, could be explained by assuming a lower level of the water table (600 m) during fluid inclusion formation (see Fig.3a). Furthermore, in order to explain the boiling process at a depth of 1001 m (which has comparable temperature and salinity with the discharge fluid), a CO_2 content of 1 mole % (actual content of CO_2 in the discharge fluid) can be taken in to consideration (see Fig. 3a) . However, in case of well LA-7 comparison of the T_h with the B.P.C.W reveals that all secondary inclusions with higher homogenization temperature fall along the B.P.C.W, indicating that the hydrothermal fluid in this part of the field was close to boiling at the time of trapping of these inclusions fluids.

(c) Well LA-8

In well LA-8, all the range and average T_h values of the secondary inclusions, in calcite and quartz crystals, appear to be almost in line with the present measured temperature, indicating a stable thermal regime after fluid inclusion formation. However, the range and average T_h values for primary inclusion in calcite crystal at a depth of 2500 m are higher than those of the secondary inclusions and the present in-hole temperature (see Fig. 3c), indicating the circulation of high-temperature fluids in the past. As a consequence, evidence of cooling is registered in this zone. This cooling process is also supported by the occurrence of low temperature clay mineral assemblages as replacement of the high temperature calc silicate minerals (Teklemariam et al., 1996).

The high temperature fluid responsible for the formation of these primary inclusions (Fig.3c) in calcite crystal could also possibly be responsible for the propylitic type of alteration.

The presence of both liquid-rich and vapour-rich inclusions in some of these samples suggest that at the time of growth of the host crystals, the hydrothermal fluids in these parts of the field were close to boiling. Most of the Th values recorded in well LA-8 fall in the liquid field with respect to the B.P.C.W. In order to explain the boiling processes at depths of 1050 m and 2050 m, we can assume a lower level of water table (800 m) during the fluid inclusion formation. Further lowering of the water table (1200 m) could possibly be an explanation for the occurrence of boiling during the entrapment of inclusion fluid at a depth of 1964 m. On the other hand, the secondary inclusion fluid in calcite at depths of 1050 m and 2500 m could possibly be derived from the fluid formed as a result of dilution/mixing process. This dilution process could be between the ascending boiled fluid and inflow of cold meteoric water accompanied by a rise in the level of the water table (800 m). It is interesting to note that, the average homogenization temperatures (240°C) at depths of 1050 and 2500 m (secondary inclusions in calcite) are in close agreement with the present temperature (250 °C) of the discharge fluid (Fig.3c).

3.4 T_{mi} - T_h relationships

The T_{mi}-T_h distribution (Fig.4) indicates the occurrence of both boiling and mixing processes in the Aluto-Langano geo-thermal system. The range and average of all T_{mi} and T_h data have been plotted on T_{mi}-T_h diagram in order to assess the boiling and mixing relations from fluid inclusion data (Fig. 4).

The production wells of Aluto have a fluid with total molality of dissolved salts (Na+K+Ca+Cl+...) of about 0.04-0.07 m (0.1-0.2 wt % NaCl eq.), where CO_2 is in the range of 0.1 to 0.5 m (Table 1). This means that CO_2 will contribute from 2 to 7 times as much to the T_{mi} as will the salts. Hence, boiling and consequent gas loss would have a large effect on T_{mi}. T_h and T_{mi} data from the Aluto fluid inclusions can be interpreted in terms of a boiling (and gas loss) and a dilution trend, just as in the chloride-enthalpy diagram for the present day fluids. Samples plotted between the two end member trends indicate that both boiling and dilution processes have occurred. Since boiling and mixing are the dominant process in geothermal systems, a combination of these processes should account for most of the variation in the data (Fig.4).

As is shown in the figure, fluid inclusion data from Aluto wells fit along two apparent trends. One is dilution from higher to lower temperature water passing through (no.9 & no.5) and the other is a boiling curve (gas loss; Fig. 4). The rest of the data enveloped by the curves for the two end members (boiling and dilution), indicates that these inclusion fluids are formed as a result of both dilution and boiling processes. The range and average value of T_h and T_{mi} data for secondary inclusions of well LA-7 (798 m) and for primary inclusions of well LA-4 (1001 m) could possibly be explained due to a continous boiling process accompanied by a temperature drop and increment of salinity.

SUMMARY OF RESULTS

In the upflow zone (wells LA-3 and LA-6), a comparison between the homogenization temperature of fluid inclusions and the in-hole temperature indicates a heating up of the fluid. Besides, the above studies indicate that both CO_2 content and salinity have changed considerably with time from early hydrothermal fluid circulation up to now. This process might be due to an intake of a CO_2 rich, high enthalpy superheated fluid to the system. On the other hand, the physical and chemical evolution of the system in the zone lateral outflow, including well LA-8, can be described in terms of two stages as follows:

(1) The first stage was characterized by the boiling of a high temperature fluid represented by primary and pseudosecondary inclusions in calcite and by the highest temperature inclusions in quartz (see Figs.3a-c). The vapour-rich inclusions were trapped in quartz crystals during this stage. Boiling accompanied by mixing processes were also deduced from the T_h-T_{mi} trend in Aluto wells (Fig.4). Continous boiling process caused the cooling of the fluid and increasing of its salinity (e.g. 1001 m (LA-4) ;798 m (LA-7)). In the mean time, boiling of fluids may be responsible for the lowering of water table in low permeability conditions. The high- temperature calc-silicate + calcite alteration assemblage may be related to this stage of the geothermal activity.

(2) The second stage was dominated by the invasion of meteoric water which mixed with the ascending boiled fluids. The mixing process may be caused by an increasing of permeability which have connected the surface aquifer with the deep geothermal system. The incursion of the meteoric water quenched the boiling of the deep hot fluids and may have led to the rising of the water table. This cooling process is in good agreement with the presence of low temperature clay alteration mineral assemblage as the replacement of the calc-silicate assemblage.

ACKNOWLEDGEMENTS

This research work was financially supported by CNR (National Research Council of Italy). The author is indebted to the EIGS for granting permission to undertake this research abroad. My grateful thanks are also extended to Dr. Giovanni Ruggieri for his guidance and suggestions in the analysis and interpretation of fluid inclusion studies.

REFERENCES

Gianelli, G. and Teklemariam, M. (1993). Water-rock interaction processes in the Aluto-Langano geothermal field (Ethiopia). J. Volc. Geotherm. Res. 56, 429-455.

Haas, J.L., Jr. (1971) . The effect of salinity on the maximum thermal gradient of a geothermal system at hydrostatic pressure. Econ. Geol., 66, pp. 940-946.

Hedenquist, J.W., and Henley, R.W. (1985). The importance of CO_2 freezing point measurements of fluid inclusions: Evidence from active geothermal systems and implication of epithermal ore deposition. Econ. Geol. V.80.pp 1379-1406.

Hedenquist, J. W. (1990). The thermal and geochemical structure of the Broadlands-Ohaaki geothermal system, New Zealand. Geothermics, 19. pp.151-185.

Poty, B., Leory, J., Jachimowicz, L. (1976). Un nouvel appareil pour la mesure de temperatures sous le microscope, l'installation de microthermometrie CHAIXMECA. Bull.Soc. Fr. Mineral. Cristallogr., V.99.pp. 182-186.

Reyes, A.G,. (1990). Petrology of Phillipine geothermal systems and the application of alteration mineralogy to their assessment. Jour. Volc. Geoth. Res. 43, pp. 279-309.

Roedder, E. (1970). Application of an improved crushing microscope stage to studies of the gases in fluid inclusions. Schweiz. Mineral. Petrogr. Mitt., V.50. pp. 41-58

Sasada, M. (1985). CO_2 bearing fluid inclusions from geothermal fields. Geotherm. Res. Council Trans, 9, pp.351-356.

Sasada, M., Roedder, E., Belkin, H.E. (1986). Fluid inclusions from drillhole DW-5, Hohi geothermal area Japan: Evidence of boiling and procedure for estimating CO_2 content. J. Volc. Geoth. Res. V.30. pp. 231-251.

Taguchi, S. And Hayashi, M. (1983). Past and present subsurface structures of the Krishma geothermal area, Japan. Trans. Geoth. Res. Counc, 7, pp. 199-203.

Teklemariam, M. (1996). Water-rock interaction processes in the Aluto-Langano geothermal field, Ethiopia. Department of Earth Sciences, University of Pisa. Ph.D thesis. pp. 295.

Teklemariam, M., Battaglia, S., Gianelli, G., and Ruggieri, G. (1996). Hydrothermal alteration in the Aluto-Langano geothermal field, Ethiopia.Geothermics,25, No. 6.pp679-702.

Valori, A., Teklemariam, M., and Gianelli, G. (1992). Evidence of temperature increase of CO_2-bearing fluids from Aluto-Langano geothermal field, Ethiopia: A fluid inclusion study of deep wells LA-3 and LA-6. Eur. J. Mineral. 4, pp.907-919.

Figure 1. Location map of the Ethiopian Rift Showing the main hydrothermal manifestations and the Aluto-Langano geothermal field (After Gianelli and Teklemariam, 1993; modified).

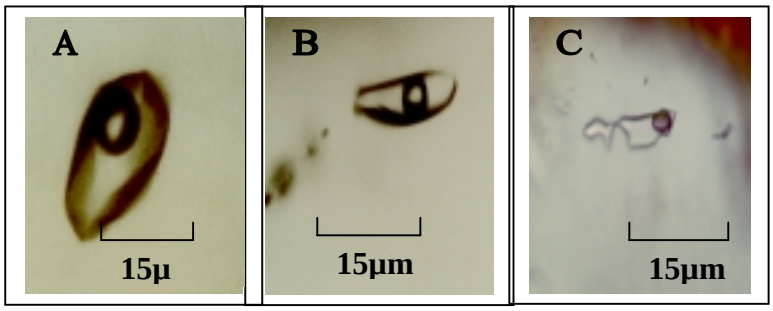

Figure 2. Photo-micrograph of (a) Primary liquid rich inclusions in hydrothermal quartz from well LA-4, 1001 m; (b) Secondary liquid rich inclusions in hydrothermal quartz crystal from well LA-3, 1150 m; (c) Secondary vapour rich inclusions in magmatic quartz crystal from well LA-3, 1779 m.

WELL	**LA-3**	**LA-4**	**LA-6**	**LA-6**	**LA-8**
TEMP (°C)	**320**	**233**	**335**	**226**	**270**
Na	661	991	733	806	821
K	150	17.4	199	103	131
Ca	0.26	12.4	0.19	1.06	0.22
Mg	0.04	0.65	0.03	0.19	1.06
SO4	121	145	102	30.6	38.8
Cl	277	645	476	334	398
F	41	56	40.7	30.6	40.7
Tot.mol (el)	0.04	0.07	0.05	0.05	0.05
Tmi-cc (el)	-0.07	-0.12	-0.09	-0.08	-0.1
SiO_2	437	265	567	294	387
H_2S	86.7	6.46	230.2	230.2	21.76
CO_2	4880	22079	11220	11149	5786
Tot.mol (n.el)	0.12	0.5	0.27	0.26	0.14
Tmi-cc (n.el)	-0.22	-0.94	-0.5	-0.48	-0.26

Table1. The total molality and contribution to Tmi for electrolytes (el) and non electrolytes (n.el). Tmi-cc = Data calculated from the electrolytes and non-electrolytes. Total discharge compositions (in ppm) of Aluto wells from which fluid inclusion samples were available for examination are also reported.

WELL	DEPTH (M)	HOST MINERAL	FLUID.I TYPE	Th (ºC)	Tmi (ºC)	BUBBLE BEHAVIOUR	CO_2 content Mol %	wt %
LA-3	850	Cc	S	259	-0.4	collapsed	<0.08	<0.20
	850	Cc	S	244	-	collapsed	<0.08	<0.20
	850	Cc	S	270	-0.4	collapsed	<0.08	<0.20
	850	Cc	S	270	-1.2	collapsed	<0.08	<0.20
	1150	Qz	S	243	-1	expanded	>0.15	>0.37
	1150	Qz	S	285	-0.7	Shrunk?	<0.09	<0.22
LA-4	1001	Qz	P	274	-0.5	expanded	>0.16	>0.38
	1001	Qz	P	278	-0.5	collapsed	<0.09	<0.21
	1001	Qz	P	268	-0.5	expanded	>0.16	>0.38
LA-6	1304	Cc	S	298	-1	collapsed	<0.09	<0.22
	1304	Cc	S	314	-	collapsed	<0.09	<0.24
	1304	Cc	S	297	-	expanded	>0.15	>0.37
	1508	Cc	S	287	-	collapsed	<0.08	<0.20
	1508	Cc	S	287	-	collapsed	<0.08	<0.20
LA-7	798	Qz	S	258	-1.4	expanded	>0.15	>0.37
	798	Qz	S	259	-1.3	expanded	>0.15	>0.37
	798	Qz	S	255	-1.8	expanded	>0.15	>0.37
	2040	Qz	S	267	-0.3	expanded	>0.15	>0.37
	2040	Qz	S	279	-1	expanded	>0.16	>0.38
LA-8	1964	QZ	S	211.1	-0.1	collapsed	<0.08	<0.18
	1964	Qz	S	280.9	-1.2	expanded	>0.16	>0.38
	1964	Qz	S	266.3	-0.4	expanded	>0.15	>0.37
	2500	Cc	Ps	303.4	-0.8	expanded	>0.17	>0.40
	2500	Cc	Ps	304.8	-0.8	expanded	>0.17	>0.40
	2500	Cc	Ps	306	-0.8	expanded	>0.17	>0.40

Table 2. Bubble behaviour on crushing and estimated CO2 content for inclusions from Wells LA-4, 7 and 8 and wells LA-3 and LA-6. Estimated concentration of CO2 is based on the graphical experiment of Sasada et al., 1985. Th = Homogenization temperature; Tmi = ice melting temperature; P = Primary fluid inclusion; PS = Psuedosecondary inclusion; S = secondary inclusion.

Table 3. A summary of microthermometric data (°C) from wells LA-4, 7 and 8 (present study) and from wells LA-3 and LA-6 (Valori et. al., 1992) on hydrothermal quartz (Qz) and calcite (Cc). Th= Homogenization temperature with number of measurements (n); Tms= Measured in-hoe temperature; ΔT= Tms-Average T_h; Tmi = ice melting temperature; Tm-ms = Average measured ice-melting temperature; Tm-cc = Calculated Tmi based on composition of reservoir fluid. Apparent salinity expressed as wt % NaCl eq. P=Primary; PS= Pseudosecondary; S= Secondary inclusions. M= molality

WELL	DEPTH	HOST	TYPE			Tms	ΔT	Tmi		Apparent Salinity		Tm-cc	Calc.CO_2 (m)	Actual CO_2 (m)
				Range	Average(n)			Range	Average (Tm-ms)	Range	Average			
LA-3	850	Cc	S	242-284	265 (63)	280	-15	-0.3 to –1.5	-0.9	0.5-2.6	1.5	-0.3	0.12-0.77	0.11
	1150	Qz	S	243-301	279 (32)	303	-24	-0.7 to-1.1	-0.9	1.2-1.9	1.5		0.34-0.55	
	1779	Qz	S	262-323	297(75)	314	-17	-0.2 to-1.9	-1.2	0.3-3.2	2		0.07-<0.85	
	2117	Qz	S	291-347	333(15)	315	18	-	-	-	-			
LA-4	1001	Qz	P+PS	204-280	238(53)	230	8	-0.2 to –1.4	-0.5 (53)	0.3-2.3	0.9	-1.1	0.04-0.69	0.5
		Cc	P+PS	201-246	223(36)	230	8	-0.8 to –1.1	-1.0 (35)	1.3-1.8	1.6		0.37-0.53	
	1250	Qz	P+PS	278-329	303(21)	230	73	-0.9 to –1.2	-1.0 (2)	1.5-2.0	1.7		0.42-0.58	
		Cc	S	248-264	255(5)	230	25	-0.5	-0.5(5)	0.8	0.8		0.2	
	1660	Qz	P+PS	253-309	286(14)	220	66	-0.6 to –1.1	-0.9(14)	1.0-1.8	1.4		0.26-0.53	
LA-6	1304	Cc	P	289-292	290(8)	295	-5	-0.3 to –1.0	-0.7	0.5-1.7	1.2	-0.6	0.11-0.49	0.21
		Cc	S	251-335	297(47)	295	2	0.0 to –1.3	-0.5	0.0-2.2	0.9		0.00-0.65	
	1508	Qz/Cc	P	243-345	279(56)	300	-22	-0.3 to –1.9	-0.9	0.5-3.2	1.5		0.11-<0.85	
		Qz/Cc	S	248-351	288(73)	300	-12	0.0 to –1.7	-0.6	0.0-2.9	1		0.00-<0.85	
	1764	Qz	S	255-343	308(23)	314	-6	-0.6 to –1.1	-0.9	1.1-.9	1.4		0.27-0.54	
LA-7	798	Qz	S	215-287	250(81)	210	40	-1.2 to –1.8	-1.4(76)	2.0-3.0	2.3	-0.6	0.60-<0.85	0.25
	1791	Cc	P+PS	319-335	326(81)	150	176	-0.8 to –1.3	-1.0 (23)	1.3-2.1	1.6		0.39-0.66	
	2040	Qz	S	255-334	286(50)	130	150	-0.2 to –1.5	-1.0 (50)	0.3-2.5	1.7		0.07-0.76	
LA-8	1050	Cc	S	214-238	227(11)	255	-28	-0.5 to –1.0	-0.7(11)	0.8-1.7	1.2	-0.4	0.22-0.48	0.13
	1964	Qz	S	242-315	269(89)	260	9	-0.3 to –1.3	-0.8(85)	0.5-2.1	1.3		0.11-0.65	
	2500	Cc	P+PS	292-330	309(64)	250	59	-0.4 to –1.6	-0.8(64)	0.7-2.6	1.3		0.6-0.81	
	2500	Cc	S	240-262	252(16)	250	2	-0.4 to –0.9	-0.7(16)	0.7-1.5	1.2		0.16-0.43	

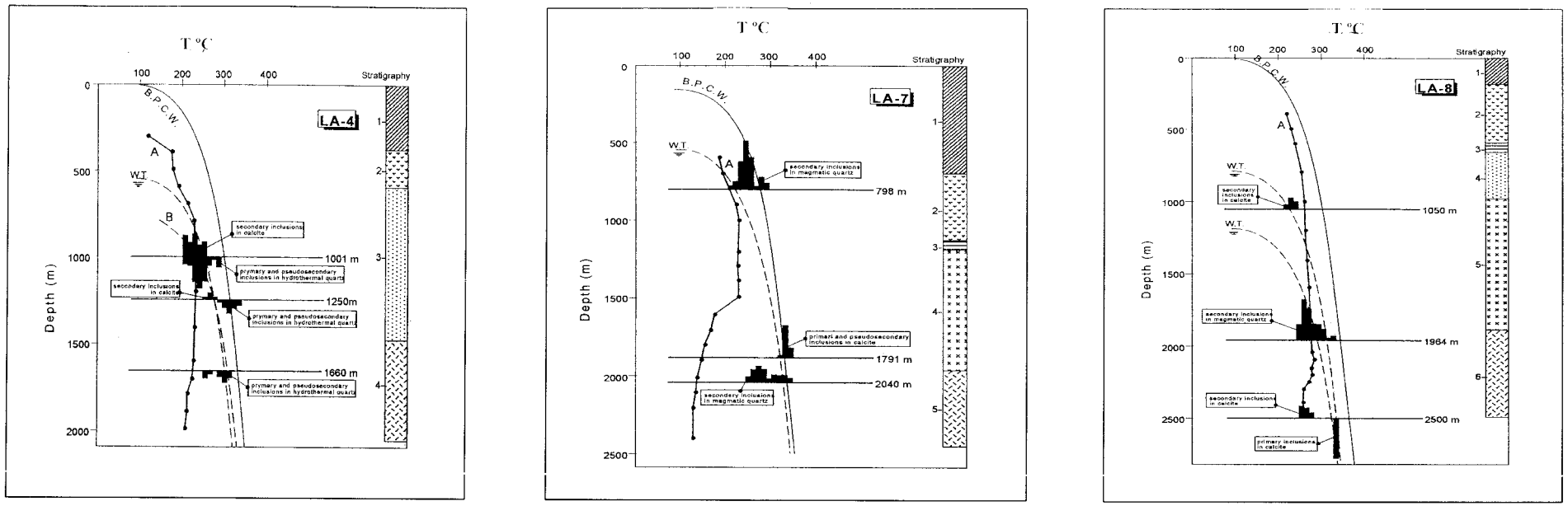

Figure 3. Stratigrapgy and comparison of T_h, boiling point curves and thermal profiles for (a) well LA-4; (b) well LA-7 ; and (c) well LA-8. A= in-hole measured temperature; B.P.C.W= Boiling point curve for pure water (Haas, 1971); B= Boiling point curve for solutions with 1 mole % of CO_2 content. Dashed line is a curve adjusted to 100°C at the current water table (W.T). Stratigraphy -Well LA-4 = 1- Recent Aluto peralkaline rhyolites and associated pyroclasics; 2- Hulo Seyno ignimbrite; 3- Bofa basalt; 4- Tertiary ignimbrite. Well LA-7 = 1 &2 same as LA-4; 3=Lake sediments; 4- Bofa basalt; 5- Tertiary ignimbrite. Well LA-8 = 1&2 same as LA-4; 3= Clastic and volcanclastic products; 4= Lake sediments; 5= Bofa basalts; 6= Tertiary ignimbrite.

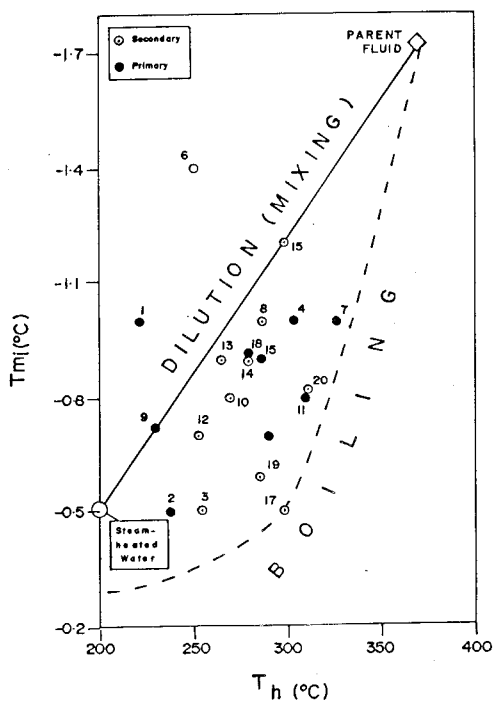

Figure 4. Homogenization temperature (T_h) versus ice melting temperature (T_{mi}) relations for primary, pseudosecondary and secondary inclusions from wells LA-3, 4, 6, 7 and 8. (1) LA-4/1001 (Calcite); (2) LA-4/1001 (Quartz); (3) LA-4/1250 (Calcite); (4) LA-4/1250 (Quartz); (5) LA-4/1660; (6) LA-7/798; (7) LA-7/1791; (8) LA-7/2040; (9) LA-8/1050; (10) LA-8/1964; (11&12) LA-8/2500; (13) LA-3/1050; (14) LA-3/1150; (15) LA-3/1779; (16 &17) LA-6/1304; (18 & 19) LA-6/1508; (20) LA-6/1764.